

Syntheses and Magnetic Properties Study of Isostructural $\text{BiM}_2\text{BP}_2\text{O}_{10}$ ($M = \text{Co}, \text{Ni}$) Containing a Quasi-1D Linear Chain Structure

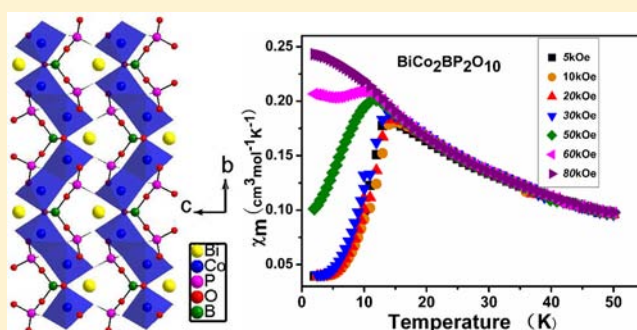
Wei-Long Zhang,[†] Zhang-Zhen He,[†] Tian-Long Xia,[‡] Zhong-Zhen Luo,[†] Hao Zhang,[†] Chen-Sheng Lin,[†] and Wen-Dan Cheng^{*,†}

[†]State Key Laboratory of Structural Chemistry, Fujian Institute of Research on the Structure of Matter, Chinese Academy of Sciences, Fuzhou 350002, People's Republic of China

[‡]Department of Physics, Renmin University of China, 59 Zhongguancun Avenue, Beijing 100872, People's Republic of China

Supporting Information

ABSTRACT: We present here the structures and magnetism of two quasi-1D linear chain compounds of $\text{BiM}_2\text{BP}_2\text{O}_{10}$ ($M = \text{Co}, \text{Ni}$), which were synthesized by traditional solid-state reactions for the first time. Two title compounds crystallize in the monoclinic system with space group $P2_1/c$ and feature novel 3D structures with a linear chain structure of $\{\text{MO}_6\}_n$ further connected by $[\text{BP}_2\text{O}_{10}]^{7-}$ anionic groups. The results of magnetic property measurements evidence the antiferromagnetic properties of both compounds in low magnetic field and a field-dependent metamagnetic transition from the antiferromagnetic to ferromagnetic ground state of the $\text{BiCo}_2\text{BP}_2\text{O}_{10}$ complex.



INTRODUCTION

Inorganic functional materials possessing low-dimensional crystal structures,¹ in particular, transition-metal oxides with a linear chain structure,² have attracted much attention in solid-state physics and chemistry since the discovery of their various fascinating magnetic and electronic phenomena. Numerous studies on 1D magnetic systems have been carried out, for example, on $S = 5/2$ Heisenberg (Mn^{2+}),³ $S = 1$ (Ni^{2+} , Haldane system),⁴ $S = 1/2$ Ising (Co^{2+}),⁵ and $S = 1/2$ Heisenberg (Cu^{2+}) systems.⁶ The magnetic anisotropy of the spin carriers is one key factor that affects the magnetic behavior of such 1D systems. If isotropic ions are employed, isotropic Heisenberg chains are to be expected, whereas if anisotropic metal ions are used, Ising chains and hence single-chain magnets can be expected. Considerable efforts have been devoted to the syntheses and investigation of linear chain structure magnetic materials with large uniaxial anisotropy because these Ising anisotropic chains offer the possibility of studying single-chain magnets (SCMs) with unique physical properties.⁷ It is a great challenge to prepare novel crystal materials with a linear chain structure.

Much research focused on the metal linear chain system based on borates, phosphates, and vanadate has been established.^{8–10} Our research of the borophosphates has led to some new borophosphate compounds with quite different structures.¹¹ Borophosphates have rich structural chemistry.^{12–14} We started to focus on metal borophosphate compounds to find some with a linear chain structure of

transition metals. There is very scant information about quaternary or quinary anhydrous systems containing transition metals, and only $\text{M}^{\text{III}}_2\text{BP}_3\text{O}_{12}$ ($M = \text{Fe}, \text{In}, \text{Cr}, \text{V}$),¹⁵ Co_3BPO_7 ,¹⁶ $\text{Co}_3\text{BP}_3\text{O}_{14}$,¹⁷ and KZnBP_2O_8 ¹⁸ have been reported. Recently, we have investigated transition-metal borophosphate compounds of quaternary systems including Bi. Bi^{3+} cations have a large ionic radius and are able to exhibit several types of asymmetric coordination geometry as a result of the existence of stereochemically active lone pair electrons, which may act as a “chemical scissors”.^{19,20}

Guided by this idea, two new quinary compounds, namely, $\text{BiM}^{\text{II}}_2\text{BP}_2\text{O}_{10}$ ($M = \text{Co}, \text{Ni}$) with a quasi-1D linear chain structure, have been successfully synthesized by traditional solid-state methods. Herein, in this study, we first report on the syntheses, structures, and magnetic properties of $\text{BiM}^{\text{II}}_2\text{BP}_2\text{O}_{10}$ ($M = \text{Co}, \text{Ni}$).

EXPERIMENTAL SECTION

Materials and Instrumentation. All of the chemicals were analytically pure from commercial sources and used without further purification. $\text{NH}_4\text{H}_2\text{PO}_4$ (AR), H_3BO_3 (AR), $\text{CoC}_2\text{O}_4 \cdot 2\text{H}_2\text{O}$ (AR)/ $\text{C}_4\text{H}_6\text{CoO}_4 \cdot 4\text{H}_2\text{O}$ (AR), $\text{Ni}(\text{HCO}_2)_2 \cdot 2\text{H}_2\text{O}$ (PR)/ $\text{NiC}_2\text{O}_4 \cdot 5\text{H}_2\text{O}$ (AR), and Cs_2CO_3 (AR) were purchased from Shanghai Reagent Factory. Single crystals of the title compounds were selected for indexing and intensity data collection on a Rigaku Mercury CCD diffractometer or an SCXmini diffractometer at 293 K. The structures were solved by

Received: April 13, 2012

Published: August 1, 2012

the direct methods and refined anisotropically by using SHELXS-97. Microprobe elemental analyses were performed by using a field emission scanning electron microscope (FESEM, JSM6700F) equipped with an energy-dispersive X-ray spectroscope (EDS, Oxford Inc). The XRD patterns were recorded on a MiniFlex2 goniometer with Cu K α radiation (30 kV, 15 mA) in the continuous scanning mode, and the 2θ scan range was from 5° to 85° in steps of 0.2°. Thermogravimetric analyses (TGA) and differential thermal analyses (DTA) were carried out with a NETZSCH STA 449C unit under an air atmosphere. The samples were placed in Al₂O₃ crucibles and heated from 35 to 1200 °C at the rate of 10.0 °C/min. Magnetic susceptibility measurements for the two compounds were performed with a PPMS magnetometer. The raw data were corrected for the susceptibility of the container and the diamagnetic contributions of the sample using Pascal constants.

Synthesis of BiM^{II}BP₂O₁₀ (M = Co, Ni). Compound BiCo₂BP₂O₁₀ was synthesized by solid-state reaction. A powder mixture of 0.0890 g of Cs₂CO₃, 0.6481 g of Bi₂O₃, 0.3831 g of CoC₂O₄·2H₂O, 0.3381 g of NH₄H₂PO₄, and 0.2991 g of H₃BO₃ was first ground in an agate mortar and then transferred to a platinum crucible. The sample was gradually heated in air at 573 K for 6 h to decompose H₃BO₃ and NH₄H₂PO₄ and finally heated at 1233 for 24 h. The intermediate product was slowly cooled to 1073 K at a rate of 2 K/h, where it was kept for 10 h and then quenched to room temperature. Some violet crystals of different shapes were mechanically removed from the solidified flux. The synthesis of a single crystal of compound BiNi₂BP₂O₁₀ was carried out using the powder mixture of 0.0829 g of Cs₂CO₃, 0.6490 g of Bi₂O₃, 0.3295 g of Ni(HCO₂)₂·2H₂O, 0.3851 g of NH₄H₂PO₄, and 0.2946 g of H₃BO₃. Some light yellow block crystals were selected carefully from the sintered product for the single-crystal detection. After structural analysis, the red and yellow crystalline powder samples of the two title compounds were then obtained quantitatively by the reaction of a mixture of Bi₂O₃, C₄H₆CoO₄·4H₂O/Ni(HCO₂)₂·2H₂O, H₃BO₃, and NH₄H₂PO₄ in a molar ratio of 1:4:2:4 at 1123 K/1193 K for 30 h, respectively. The purities of the compounds were confirmed by XRD powder diffraction studies (Figure S1, see Supporting Information).

Single-Crystal Structure Determination. Single crystals of the title compounds were selected for indexing and intensity data collection on a Rigaku Mercury CCD diffractometer (BiCo₂BP₂O₁₀)/SCXmini diffractometer (BiNi₂BP₂O₁₀) at 293 K, respectively. Absorption corrections by the multiscan method were applied for both of them,²¹ and both structures were solved by the direct method and then refined on F^2 by the full-matrix least-squares method, with the SHELXL/PC programs.²² All atoms were refined with anisotropic thermal parameters. Crystallographic data and structural refinements for the two title compounds are summarized in Table 1. The atomic coordinates are listed in Table S1 (see Supporting Information), and important bond distances and angles are listed in Table S2. The final refined solutions obtained were checked with the ADDSYM algorithm in the program PLATON,²³ and no higher symmetry was found. In order to confirm the chemical composition of the compounds, we performed microprobe elemental analyses of the single crystals, indicating the presence of Bi, Co, and P elements in a molar ratio of 4.6:10.3:9.1 in compound BiCo₂BP₂O₁₀ and Bi, Ni, and P in a molar ratio of 4.0:7.2:11.7 in compound BiNi₂BP₂O₁₀ (Figure S3, see Supporting Information). Since the samples were unpolished and X-ray corrections may be approximate especially for light elements, the EDS results were in agreement with those from single-crystal X-ray structural analyses. ICSD Nos. 423963 and 423964 contain the supplementary crystallographic data for this paper. The data can be obtained from the Fachinformationszentrum Karlsruhe, 76344 Eggenstein-Leopoldshafen, Germany (fax: (49) 7247-808-666; e-mail: crysdata@fz-karlsruhe.de).

RESULTS AND DISCUSSION

In order to search for new compounds within a linear chain structure and better understand the crystal structures and their magnetic properties, exploration on the transition-metal

Table 1. Crystal Data and Structural Refinements for Compounds 1 and 2

	compound 1	compound 2
formula	BiCo ₂ BP ₂ O ₁₀	BiNi ₂ BP ₂ O ₁₀
fw	559.59	559.11
space group	<i>P</i> 2(1)/ <i>m</i> (No. 14)	<i>P</i> 2(1)/ <i>m</i> (No. 14)
<i>a</i> , Å	5.0782(9)	5.0682(13)
<i>b</i> , Å	11.2889(10)	11.282(3)
<i>c</i> , Å	6.4020(11)	6.322(2)
α , deg	90	90
β , deg	107.827(9)	90
γ , deg	90	90
<i>V</i> , Å ³	349.39(9)	345.79(17)
<i>Z</i>	2	2
<i>D</i> _{calcd} g·cm ⁻³	5.319	5.370
μ , mm ⁻¹	30.323	31.286
GOF on F^2	1.113	1.052
R1, wR2 [$I > 2\sigma(I)$] ^a	0.0195, 0.0470	0.0258, 0.0611
R1, wR2 (all data)	0.0206, 0.0473	0.0272, 0.0620

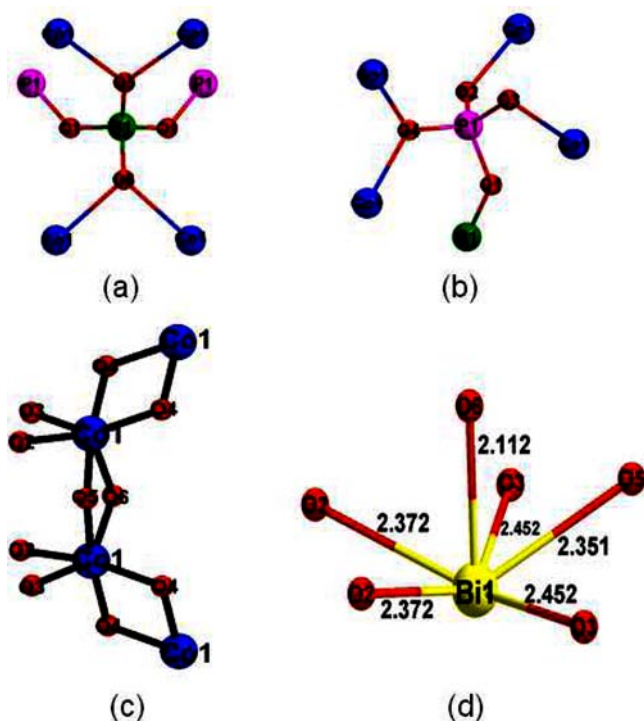
$$^a R1 = \frac{\sum |F_o| - |F_c|}{\sum |F_o|}, wR2 = \left\{ \frac{\sum w[(F_o)^2 - (F_c)^2]^2}{\sum w(F_o)^2} \right\}^{1/2}$$

borophosphate compounds afforded two new quinary compounds, namely, BiM^{II}BP₂O₁₀ (M = Co, Ni) by traditional solid-state methods. The two title compounds feature novel 3D structures with a linear chain structure of {MO₆}_n further connected by [BP₂O₁₀]⁷⁻ borophosphate anionic groups.

Structural Descriptions. X-ray analysis revealed that the compounds BiM^{II}BP₂O₁₀ (M = Co, Ni) are isotypic and crystallize in the monoclinic system with space group *P*2₁/*c*. Since they are isostructural, only the structure of BiCo₂BP₂O₁₀ will be discussed in detail as a representative.

The asymmetric unit of BiCo₂BP₂O₁₀ consists of one bismuth ion, one cobalt ion, and one borophosphate anionic group, [BP₂O₁₀]⁷⁻. All of the atoms represent independent crystallographic sites. As seen from Scheme 1a, the B atom is tetrahedrally coordinated by four oxygen atoms, forming a BO₄ tetrahedron geometry with B–O bond lengths ranging from 1.456(9) to 1.478(6) Å (Table S2, see Supporting Information). Each BO₄ tetrahedral geometry shares two corners with two different PO₄ tetrahedra to form the [BP₂O₁₀]⁷⁻ borophosphate anionic group and uses two other corners to connect with four [CoO₆] octahedra. Hence, each BO₄ tetrahedral group is hexacoordinate with two PO₄ tetrahedra and four [CoO₆] octahedra. Scheme 1b shows that each P atom is also coordinated by four oxygen atoms in a tetrahedral geometry with P–O bond distances ranging from 1.520(4) to 1.553(4) Å (Table S2, see Supporting Information). The longest P–O distances are found from the P–O–B linking (1.553(4) Å), and the distances of P–O bonds within the P–O–Co linking are 1.520(4) and 1.543(4) Å. Each PO₄ tetrahedral group acts as pentacoordinate with one BO₄ tetrahedron and four [CoO₆] octahedra (Scheme 1b). Co1 is connected by six oxygen atoms to form a little distorted octahedral geometry with the Co–O distances ranging from 2.066 to 2.207 Å (Table S2, see Supporting Information). The most remarkable structural feature is that magnetic Co²⁺ ions have independent crystallographic sites with the arrays of edge-shared CoO₆ octahedra forming quasi-1D linear chains along the *b*-axis, and the skew chains are separated by nonmagnetic [BP₂O₁₀]⁷⁻, resulting in a quasi-1D structural arrangement, which also can be seen from Figure 1a. The neighboring

Scheme 1. Coordination Modes of the Anion Group in $\text{BiCo}_2\text{BP}_2\text{O}_{10}$ ^a



^aBi, Co, P, B, and O atoms are represented by yellow, blue, pink, dark green, and red circles respectively.

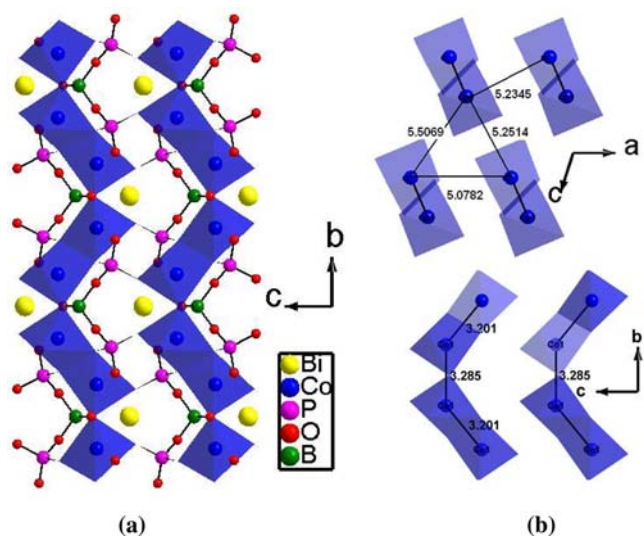


Figure 1. View of the structure of $\text{BiCo}_2\text{BP}_2\text{O}_{10}$ along the a -axis (a); selected $\text{Co}\cdots\text{Co}$ distances within the chain and between chains (b). Bi, Co, and O atoms are represented by yellow, blue, and red circles, respectively.

$\text{Co}\cdots\text{Co}$ separations between a pair of edge-sharing CoO_6 octahedra chains are in the range 3.201(2)–3.285(1) Å, and the shortest interchain $\text{Co}\cdots\text{Co}$ separation is 5.078(2) Å (Figure 1b). The metal bismuth ions are located inside the tunnels formed by the corner sharing of the $[\text{Co}_2\text{O}_{10}]$ dimer and $[\text{BP}_2\text{O}_{10}]^{7-}$ borophosphate anionic groups. The bismuth ions are surrounded by six oxygen atoms at Bi–O distances less than 3.3 Å (Table S2). The coordination polyhedron of Bi^{3+} can be better characterized by one short Bi–O bond (2.112 Å)

and five longer ones (2.351–2.452 Å) (Table S2, see Supporting Information). For Bi ions, all the oxygen atoms are located on the same side with respect to bismuth (Scheme 1d), showing for this cation a rather strong stereoactivity. It is well established that Bi^{3+} ions often generate distorted structures due to the electrostatic effect of the lone pair of electrons and act as “chemical scissors”.

Many borophosphate compounds known to date are systematically classified in terms of reviews by R. Kniep et al.^{12,13} To further understand the structure, we have employed Kniep’s concept and nomenclature of borophosphate fundamental building units (FBUs) to analyze the borophosphate partial structures of the two title compounds. As far as we know, there are two main classification criteria of borophosphate compounds: one is the ratio of borate to phosphate in borophosphate anions, and the other is disassembling the anionic partial structure into its fundamental building units. So the FBU of the borophosphate partial structure of $\text{BiCo}_2\text{BP}_2\text{O}_{10}$ is $[\text{BP}_2\text{O}_{10}]^{7-}$ with B:P = 1:2, $3\square:3\square$ (\square represents BO_4 and PO_4 tetrahedra).

TGA indicated that the compounds $\text{BiM}^{\text{II}}\text{BP}_2\text{O}_{10}$ ($M = \text{Co}, \text{Ni}$) are thermally stable up to the high temperature (Figure S2, see Supporting Information). There are no obvious steps of weight loss before 1100 °C in the curves of TGA. For the two title compounds, the total weight losses are 9.6% and 5.5% at 1200 °C, respectively, which is also confirmed by the DTA curve. The weight loss corresponds to the decomposition of the compound. The two title compounds, in which the four oxygen atoms around the B atoms are all further connected by other atoms, have higher thermal stability, which also can be seen in other anhydrous borophosphates, such as KMfBP_2O_8 ($M = \text{Sr}, \text{Ba}$),¹⁴ and $\text{Sr}_6\text{BP}_5\text{O}_{20}$.²⁴

Magnetic Properties. Magnetic susceptibilities of $\text{BiM}^{\text{II}}\text{BP}_2\text{O}_{10}$ ($M = \text{Co}, \text{Ni}$) were measured at a field of 1000 Oe over a temperature range of 2–300 K. The temperature dependences of dc magnetic susceptibility and the corresponding reciprocal susceptibility of the polycrystalline material are shown in Figure 2. For compound $\text{BiCo}_2\text{BP}_2\text{O}_{10}$, the susceptibility exhibits a sharp peak around 13 K, indicative of a long-range antiferromagnetic ordering. A Curie–Weiss fit to the high-temperature susceptibility data (15–300 K) yields a Curie constant C of 7.54(4) emu K/mol and a Weiss constant θ of $-57.33(2)$ K (Figure 2a). For compound $\text{BiNi}_2\text{BP}_2\text{O}_{10}$, the magnetic susceptibility seems to be the same as that for $\text{BiCo}_2\text{BP}_2\text{O}_{10}$, and the susceptibility exhibits a sharp peak at 7.0 K. A typical Curie–Weiss behavior is observed, giving the Curie constant $C = 2.89(1)$ emu K/mol and Weiss constant $\theta = -20.46(2)$ K, as shown in Figure 2b. The negative Weiss temperature indicates antiferromagnetic exchange between transition-metal ions. The effective magnetic moment of Co^{2+} and Ni^{2+} ions in the system is calculated to be 5.49(2) and 3.40(1) μB , respectively, while the values obtained from Co^{2+} ($S = 3/2$) ions and Ni^{2+} ($S = 1$) for spin-only magnetic moments with a g factor of 2 are 3.87 and 2.82 μB , respectively. It is indicated that Co^{2+} ions have a high spin state and a higher value than is presumably due to the orbital contribution, which is very typical for octahedrally coordinated Co^{2+} .²⁵ For the Ni^{2+} compound, the effective magnetic moment μ_{eff} is 3.40(1) μB , a little larger than the theoretical value 2.82 μB , assuming that the Ni(II) ion in the octahedral environment also has a small orbital contribution to the total magnetic moment.²⁶

To estimate the exchange coupling within the $[\text{MO}_6]_n$ chain via edge-sharing, the $\chi_m T$ data can be fitted by an infinite-chain

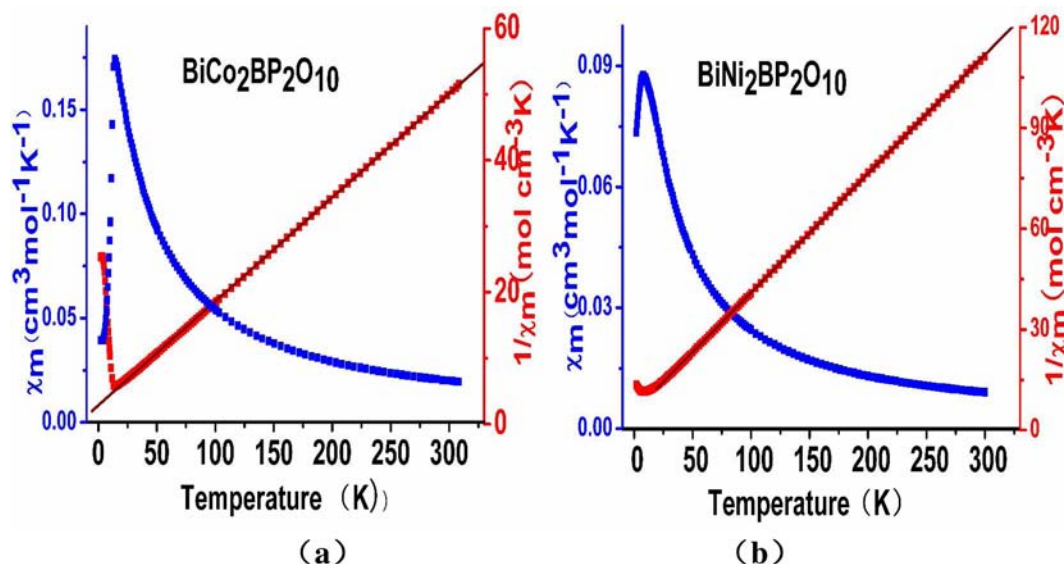


Figure 2. $1/\chi$ vs T and χ vs T plots for BiCo₂BP₂O₁₀ (a) and BiNi₂BP₂O₁₀ (b). The dark red line represents the linear fit of data according to the Curie–Weiss law.

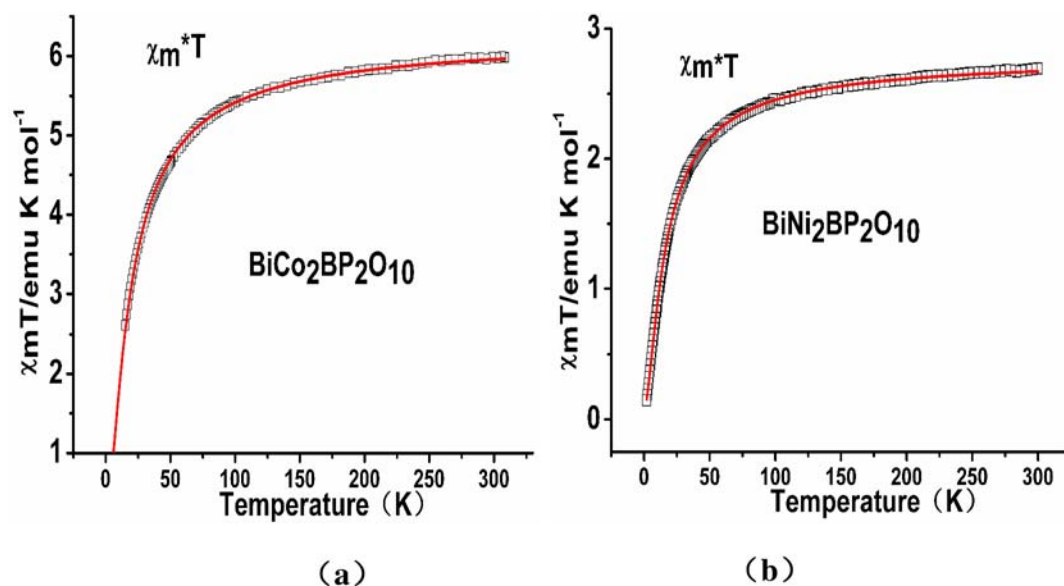


Figure 3. Temperature dependence of $\chi_m T$ for compound for BiCo₂BP₂O₁₀ (a) and BiNi₂BP₂O₁₀ (b). The circles correspond to the experimental data. The simulation is depicted as a red line by using a 1D Fisher model.

model of classical spins developed by Fisher with $H = -2J\sum S_i S_{i+1}$.²⁷ The corresponding analytical expression for the $\chi_m T$ product is listed as follows (eqs 1 and 2).

$$\chi_m T = \frac{Ng^2\beta^2 S(S+1)}{3k} \frac{1+u}{1-u} \quad (1)$$

$$u = \coth\left[\frac{JS(S+1)}{kT}\right] - \left[\frac{kT}{JS(S+1)}\right] \quad (2)$$

where N , g , β , and k have their usual meanings and J is the superexchange coupling constant between adjacent Co(II) ions.

As shown in Figure 3a, the susceptibility of BiCo₂BP₂O₁₀ above 14 K can be fitted well with $J/k_B = -5.75$ K and $g = 3.65$, and the agreement factor defined by $R = \sum(\chi_m T_{\text{exp}} - \chi_m T_{\text{cal}})^2 / \sum(\chi_m T_{\text{exp}})^2$ is 6.5×10^{-4} . Figure 3b shows that the

susceptibility of BiNi₂BP₂O₁₀ in the whole temperature range can be fitted well with $J/k_B = -5.15$ K and $g = 2.44$, and the agreement factor defined by $R = \sum(\chi_m T_{\text{exp}} - \chi_m T_{\text{cal}})^2 / \sum(\chi_m T_{\text{exp}})^2$ is 6.0×10^{-5} . The negative J suggests an antiferromagnetic interaction within the chain.²⁸

As shown in Figure 4, the behaviors of magnetization (M) as a function of applied field (H) at 2.5 K for the Co compound and at 2 K for the Ni compound are quite different. For the Co compound, dc magnetization was measured at various applied fields up to 140 kOe, and a linear behavior of magnetization is seen below 48 kOe, which is in good agreement with the AF ground state in the system, while a sudden increase appears above ~ 48 kOe, displaying a hysteresis loop with a large coercive field ($H = 48$ –140 kOe) (Figure 4a), which indicates a metamagnetic transition from the antiferromagnetic to ferromagnetic ground state. For the Ni compound, magnet-

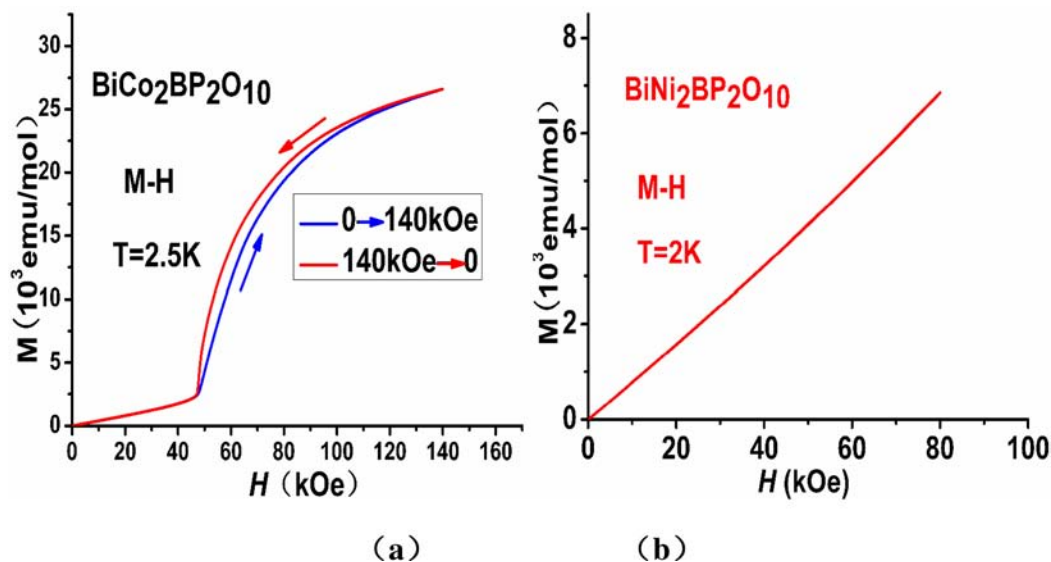


Figure 4. Magnetization (M) as a function of magnetic field (H) for $\text{BiCo}_2\text{BP}_2\text{O}_{10}$ (a) and $\text{BiNi}_2\text{BP}_2\text{O}_{10}$ (b).

ization isotherms obtained at 2 K follow a linear variation in the whole range of the magnetic field strength (0–80 kOe), and the high value of magnetization attained at higher fields ($M = 6.85 \times 10^3$ emu/mol, at 80 kOe) indicates that the Ni compound is a canted antiferromagnet (Figure 4b), which agrees with the Heisenberg-like behavior of Ni magnetic moments.

To gain further insight into a field-induced metamagnetic transition in $\text{BiCo}_2\text{BP}_2\text{O}_{10}$, magnetic susceptibilities were measured at various applied fields (H) over a temperature range of 2–50 K. As shown in Figure 5, when the applied field

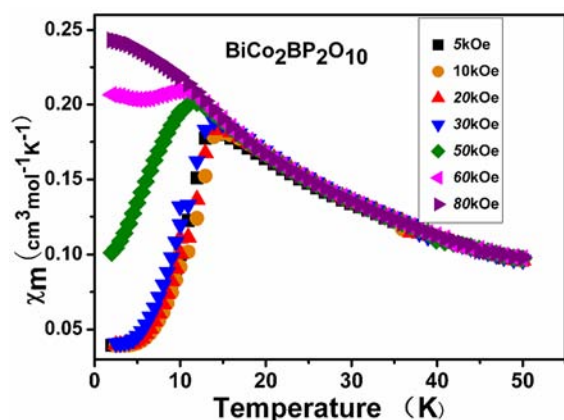


Figure 5. Magnetic susceptibilities at different applied field ($H = 5, 20, 30, 50, 60, 80$ kOe) over a temperature range of 2–50 K.

H was below 50 kOe, a sharp peak is clearly observed at 13.0 K, indicative of 3D Neel temperature (T_N). With increasing the field over 50 kOe, the susceptibility below 5 K increases rapidly and T_N shifts slightly to a lower temperature. The results are in good agreement with a metamagnetic transition from the antiferromagnetic to ferromagnetic ground state induced by an applied field.

A more convincing argument for the different nature of magnetism in the Co- and Ni-containing compounds was presented. It is clear that both compounds display a similar AF ground state due to the fact that magnetic ions (Co or Ni) have

a similar spin–lattice with a linear chain structure. The Ni^{2+} (d^8 , $t_{2g}^6 e_g^2$) ions have weak spin–orbital coupling in an octahedral environment, and the Ni compound is likely a canted antiferromagnet, which agrees with the Heisenberg-like behavior of Ni magnetic moments. Co^{2+} (d^7 , $t_{2g}^5 e_g^2$) has a larger orbital moment contribution octahedrally coordinated by oxygen atoms; thus it is reasonable that a field-dependent metamagnetic transition from the antiferromagnetic to ferromagnetic ground state can be observed, which agrees with the fact that cobalt oxides usually exhibit large magnetic anisotropy and also show interesting field-induced magnetic transitions.^{5a,29}

CONCLUSION

In summary, two new anhydrous borophosphate compounds generally formulated as $\text{BiM}_2\text{BP}_2\text{O}_{10}$ ($M = \text{Co}, \text{Ni}$) containing a quasi-1D linear chain structure have been reported for the first time. The 3D network structures, borophosphate anionic groups, and the stereochemical activity of the Bi^{3+} lone pair have also been discussed. As evidenced by magnetization measurements at low magnetic field, this framework is a strong antiferromagnet due to adjacent magnetic coupling interactions within edge-bridged chains, and the $\chi_m T$ data can be fitted by an infinite-chain model of classical spins developed by Fisher, while there is a considerable field-induced metamagnetic transition from the antiferromagnetic to ferromagnetic ground state of the Co compound. It is expected that more borophosphates with a linear chain or low-dimensional magnetic framework structure and novel physical properties can be prepared by using similar synthetic methods in the near future.

ASSOCIATED CONTENT

Supporting Information

X-ray crystallographic files in CIF format, atomic coordinates (Table S1), selected important bond lengths (Table S2), simulated and experimental XRD powder patterns for compounds 1 and 2 (Figure S1), TGA and DTA diagrams for compounds 1 and 2 (Figure S2), and results of the microprobe analysis (Figure S3). These materials are available free of charge via the Internet at <http://pubs.acs.org>.

■ AUTHOR INFORMATION

Corresponding Author

*E-mail: cwd@fjirsm.ac.cn.

Notes

The authors declare no competing financial interest.

■ ACKNOWLEDGMENTS

This investigation was based on work supported by the National Natural Science Foundation of China under the National Basic Research Program of China (No. 2007CB815307) and projects 21173225 and 21101156, Fujian Key Laboratory of Nanomaterials (No. 2006L2005), and supported by Scientific Research Foundation of President of the Chinese Academy of Sciences.

■ REFERENCES

- (1) (a) Moubah, R.; Colis, S.; Ulhaq-Bouillet, C.; Drillon, M.; Dinia, A. *J. Mater. Chem.* **2008**, *18*, 5543. (b) Moubah, R.; Colis, S.; Ulhaq-Bouillet, C.; Schmerber, G.; Viart, N.; Drillon, M.; Dinia, A.; Muller, D.; Grob, J. J. *Eur. Phys. J. B* **2008**, *66*, 315. (c) Zhang, S.-Y.; Shi, W.; Lan, Y.-H.; Xu, N.; Zhao, X.-Q.; Powell, A. K.; Zhao, B.; Cheng, P.; Liao, D.-Z.; Yan, S.-P. *Chem. Commun.* **2011**, *47*, 2859. (d) Dong, D.-P.; Liu, T.; Kanegawa, S.; Kang, S.; Sato, O.; He, C.; Duan, C.-Y. *Angew. Chem., Int. Ed.* **2012**, DOI: 10.1002/anie.201105987. (e) Kajiwara, T.; Nakano, M.; Kaneko, Y.; Takaishi, S.; Ito, T.; Yamashita, M.; Igashira-Kamiyama, A.; Nojiri, H.; Ono, Y.; Kojima, N. *J. Am. Chem. Soc.* **2005**, *127*, 10150. (f) Zheng, Y.-Z.; Xue, W.; Tong, M.-L.; Chen, X.-M.; Grandjean, F.; Long, G. J. *Inorg. Chem.* **2008**, *47*, 4077.
- (2) (a) Schiffer, P. *Nature* **2002**, *420*, 35. (b) Kodama, K.; Takigawa, M.; Horvatic, M.; Berthier, C.; Kageyama, H.; Ueda, Y.; Miyahara, S.; Becca, F.; Mila, F. *Science* **2002**, *298*, 395. (c) Coldea, R.; Tennant, D. A.; Wheeler, E. M.; Wawrzynska, E.; Prabhakaran, D.; Telling, M.; Habicht, K.; Smeibidl, P.; Kiefer, K. *Science* **2010**, *327*, 177. (d) Ritter, C.; Vorotynov, A.; Pankrats, A.; Petrakovskii, G.; Temerov, V.; Gudim, I.; Szymczak, R. *J. Phys.: Condens. Matter* **2010**, *22*, 206002. (e) Endo, T.; Doi, Y.; Wakeshima, M.; Hinatsu, Y. *Inorg. Chem.* **2010**, *23*, 10809. (f) Endo, T.; Doi, Y.; Hinatsu, Y.; Ohoyama, K. *Inorg. Chem.* **2010**, *51*, 3572.
- (3) (a) Sun, H.-L.; Wang, Z.-M.; Gao, S. *Chem.—Eur. J.* **2009**, *15*, 1757. (b) Li, W.; Barton, P. T.; Burwood, R. P.; Cheetham, A. K. *Dalton Trans.* **2011**, *40*, 7147.
- (4) Voyer, C. J.; van Lierop, J.; Ryan, D. H.; Cadogan, J. M. *J. Appl. Phys.* **2006**, *99* (8), 08H501.
- (5) (a) He, Z.-Z.; Yamaura, J.-I.; Ueda, Y.; Cheng, W.-D. *J. Am. Chem. Soc.* **2009**, *131* (22), 7554. (b) Kimura, S.; Yashiro, H.; Hagiwara, M.; Okunishi, K.; Kindo, K.; He, Z.; Taniyama, T.; Itoh, M. *J. Phys.: Conf. Ser.* **2006**, *51*, 99.
- (6) He, Z.-Z.; Lin, C.-S.; Cheng, W.-D.; Okazawa, A.; Kojima, N.; Yamaura, J.; Ueda, Y. *J. Am. Chem. Soc.* **2011**, *133* (5), 1298.
- (7) (a) Li, X.-J.; Wang, X.-Y.; Gao, S.; Cao, R. *Inorg. Chem.* **2006**, *45*, 1508. (b) Wang, S.; Zuo, J. L.; Gao, S.; Song, Y.; Zhou, H. C.; Zhang, Y. Z.; You, X. Z. *J. Am. Chem. Soc.* **2004**, *126*, 8900.
- (8) Campá, J. A.; Cascales, C.; Gutiérrez-Puebla, E.; Monge, M. A.; Rasines, I.; Ruíz-Valero, C. *Chem. Mater.* **1997**, *9* (1), 237–240.
- (9) Yang, T.; Zhang, Y.; Yang, S.-H.; Li, G.-B.; Xiong, M.; Liao, F.-H.; Lin, J.-H. *Inorg. Chem.* **2008**, *47* (7), 2562–2568.
- (10) He, Z.-Z.; Fu, D.-S.; Kyômen, T.; Taniyama, T.; Itoh, M. *Chem. Mater.* **2005**, *17* (11), 2924–2926.
- (11) Zhang, W. L.; Cheng, W. D.; Zhang, H.; Geng, L.; Li, Y. Y.; Lin, C. S.; He, Z. Z. *Inorg. Chem.* **2010**, *49*, 2550.
- (12) Kniep, R.; Engelhardt, H.; Hauf, C. *Chem. Mater.* **1998**, *10*, 2930.
- (13) Ewald, B.; Huang, Y. X.; Kniep, R. *Z. Anorg. Allg. Chem.* **2007**, *633*, 1517.
- (14) Zhao, D.; Cheng, W.-D.; Zhang, H.; Huang, S.-P.; Xie, Z.; Zhang, W.-L.; Yang, S.-L. *Inorg. Chem.* **2009**, *48*, 6623.
- (15) (a) Zhang, W.-L.; Lin, C.-S.; Geng, L.; Li, Y.-Y.; Zhang, H.; He, Z.-Z.; Cheng, W.-D. *J. Solid State Chem.* **2010**, *183*, 1108. (b) Mi, J.-X.; Zhao, J.-T.; Mao, S.-Y.; Huang, Y.-X.; Engelhardt, H.; Kniep, R.; Kristallogr., *Z. New Cryst. Struct.* **2000**, *215*, 201. (c) Meisel, M.; Paech, M.; Wilde, L.; Wulff-Molder, D. *Z. Anorg. Allg. Chem.* **2004**, *630*, 983.
- (16) Yilmaz, A.; Xianhui, B.; Kizilyalli, M.; Kniep, R.; Stucky, G. D. *J. Solid State Chem.* **2001**, *156*, 281.
- (17) Bontchev, R. P.; Sevov, S. C. *Inorg. Chem.* **1996**, *35*, 6910.
- (18) Kniep, R.; Schaefer, G.; Engelmann, H.; Boy, I. *Angew. Chem., Int. Ed.* **1999**, *38*, 3642.
- (19) Zhang, W.-L.; Cheng, W.-D.; Zhang, H.; Geng, L.; Lin, C.-S.; He, Z.-Z. *J. Am. Chem. Soc.* **2010**, *132* (5), 1508.
- (20) Zhang, W. L.; Lin, X. S.; Zhang, H.; Wang, J. Y.; Lin, C. S.; He, Z. Z.; Cheng, W. D. *Dalton Trans.* **2010**, *39*, 1546.
- (21) *CrystalClear* Version 1.3.5; Rigaku Corp.: The Woodlands, TX, 1999.
- (22) Sheldrick, G. M. *SHELXTL, Crystallographic Software Package, Version 5.1*; Bruker-AXS: Madison, WI, 1998.
- (23) Spek, A. L. *J. Appl. Crystallogr.* **2003**, *36*, 7.
- (24) Ehrenberg, H.; Laubach, S.; Schmidt, P. C.; McSweeney, R.; Knappa, M.; Mishra, K. C. *J. Solid State Chem.* **2006**, *179*, 968.
- (25) (a) Wang, X.-Y.; Sevov, S. C. *Inorg. Chem.* **2008**, *47*, 1037. (b) Wöhlert, S.; Ruschewitz, U.; Nätthe, C. *Cryst. Growth Des.* **2012**, *12*, 2715.
- (26) Berthelot, R.; Schmidt, W.; Muir, S.; Eilertsen, J.; Etienne, L.; Sleight†, A. W.; Subramanian, M. A. *Inorg. Chem.* **2012**, *51*, 5377.
- (27) Fisher, M. E. *Am. J. Phys.* **1964**, *32*, 343.
- (28) (a) Zheng, Y.-Z.; Xue, W.; Tong, M.-L.; Chen, X.-M.; Zheng, S.-L. *Inorg. Chem.* **2008**, *47*, 11202. (b) Dey, S. K.; Bag, B.; Abdul-Malik, K. M.; Salah-El-Fallah, M.; Ribas, J.; Mitra, S. *Inorg. Chem.* **2003**, *42*, 4029. (c) Jia, L.-H.; Li, R.-Y.; Duan, Z.-M.; Jiang, S.-D.; Wang, B.-W.; Wang, Z.-M.; Gao, S. *Inorg. Chem.* **2011**, *50*, 144.
- (29) (a) Kobayashi, S.; Mitsuda, S.; Ishikawa, M.; Miyatani, K.; Kohn, K. *Phys. Rev. B* **1999**, *60*, 3331. (b) He, Z.; Kyômen, T.; Taniyama, T.; Itoh, M. *Phys. Rev. B* **2005**, *72*, 172403.